

Poisson Distribution and Shoulder Structure of Charged Particle Multiplicity Distributions in Restricted Rapidity Intervals in Z^0 Hadronic Decays

Yong Chai Yi-Gang Xie
Institute of High Energy Physics, Beijing

28 Dec, 1992

1. Introduction

The properties of the charged multiplicity distribution in restricted intervals of rapidity have been studied.^[1] In this paper, we have studied the distribution in single hemisphere with restricted intervals of rapidity. The data are compared with the predictions of Lund Parton Shower model (Monte Carlo program JETSET version 6.3). We treat the distribution by Poisson which shows the independent emission of produced particles. The approach of the Poisson-like distribution in e^+e^- is different from the long-tail shape of h-h collision, this has been emphasized and argued by some theoreticians until Singapore Conference.^[2] The analysis of the shoulder structure of the multiplicity distribution in different rapidity intervals is also considered which has been observed recently.^[3]

2. Data selection and correction

This research is based on 20916 hadronic events of Z^0 decays around Z^0 peak of 91.2 GeV after selection. For event selection, we apply the same cuts as in the ALEPH papers about properties of hadronic events.^[4] The cuts are: the tracks are good only if they originate from a cylindrical region with radius $D_0 < 3\text{cm}$ and length $Z < 5\text{cm}$ around the interaction point, if they have at least four hits in TPC, if their transverse momentum P_t is larger than 200 MeV/c, if their polar angle is between 20° and 160° . Events are good only if the total energy of charged particle exceeds 15 GeV, if there are at least 5 charge tracks. if the polar angle of sphericity axis are in the range between 35° and 145° .

For correcting the multiplicity distribution, the probability matrix methods are considered:

$$T(N_{tr}) = \Sigma P(N_{tr}, N_{ob}) \times O(N_{ob})$$

where:

$O(N_{ob})$:observed reconstructed multiplicity distribution before correction
 $T(N_{tr})$:true multiplicity distribution after correction
 $P(N_{tr}, N_{ob})$:probability matrix

All the final particles of Monte Carlo truths have been treated with a life time of 1×10^{-9} sec. Those particles with its life time less than 1×10^{-9} sec are forced to decay while the others are forced to be stable. We don't consider the influence of initial radiation.

3.Results

The errors quoted after the result data are statistical errors.

1) Fig.1 gives the multiplicity distributions for different rapidity windows and Fig.2 gives the multiplicity distribution in single hemisphere for different rapidity windows. The mean multiplicities in single and both hemispheres for different rapidity windows are listed in tab.1. The following is the mean multiplicity of full space at 91Gev energy which is consistent with the ALEPH paper:^[5]

$$\langle n \rangle = 20.84 \pm 0.05$$

Tab.2 gives $\langle n \rangle / D$ defined as the ratio of mean multiplicity to distribution dispersion. We give the $\langle n \rangle / D$ in full space and the F/S defined as the ratio of $\langle n \rangle / D$ in full space to that in single hemisphere from TASSO and ours as the following^[5] :

energy	14.	22.	34.8	43.6	91.2
$\langle n \rangle / D$	3.03 ± 0.36	3.19 ± 0.41	3.28 ± 0.34	3.28 ± 0.31	3.24 ± 0.11
F/S:	1.35 ± 0.03	1.35 ± 0.03	1.34 ± 0.01	1.35 ± 0.02	1.34 ± 0.03

The value $\langle n \rangle / D$ is invariant in the range of 10%. This is consistent with the Wroblewski regulation.^[6] The curves are overlapping and they show that the multiplicity distributions with the KNO variable are independent of energy from lower energies to 91.2Gev. So we can say the scaling is still valid at 91Gev.

Compared with the data in lower energies from TASSO, this value F/S seems to be also independent with energy. It's invariant in the range of errors. Thus, in a large range of energy, the F/S approach roughly to $\sqrt{2}$ predicted by theory.^[7]

2)The results of Poisson Fit are listed in the Tab.3a, 3b, 3c, 3d. It is seen that the Poisson doesn't fit the distribution very well. The multiplicity distribution is wider than Poisson fit. This can be explained by the Barshay's opinion^[7] that introduces a parameter c related to neutral cluster. Observing the χ^2/NDF value, we get that Poisson fitting for 2-jet event multiplicity distribution is better than that of whole event multiplicity distribution in different rapidity windows by a factor of ten in χ^2/NDF value.

The theoretician paper^[8] predicts that $D^2 \propto n$ if the Poisson distribution is fully valid. For KNO scaling, $D^2 \propto n^2$. We have presented in 1) that the experimental result shows $D^2 \propto n^2$. In this point, the result is against Poisson distribution. Recently a new correction factor K from Yang-Chou Model has been introduced which is relative to the cluster size^[2]. Yang predicted that $K = D^2/n = 2$. We get $K = 1.95$ at 91Gev, which is also consistent with the prediction from Capela's paper.^[9] So we can say the experimental results support the Yang-Chou's model after modification. Observing the shape of distribution, we find that the

skewness of the distribution is positive in lower multiplicity region, and the distribution is almost symmetric around the peak. These evidences support Poisson-like shape^[8].

3) It is seen in Fig.3, Fig.4, Fig.5, that the multiplicity distributions show a sharp shoulder structure in the windows between $|y| < 1.5$ and $|y| < 2.0$; especially in the condition of single hemisphere. We analyze this shoulder structure by resolving the data into multi-jet hadronic final states, using the jet finding algorithm originally introduced by the JADE collaboration which is applied by many other collaborations for study of jet production. For each event the squares of the scaled invariant masses for each pair of charged particles i and j :

$$Y_{ij} = 2E_i E_j (1 - \cos \theta_{ij}) / E^2$$

are evaluated, Here E_i, E_j are the energies and θ_{ij} the angle between the momentum vectors of the two particles, E is the total energy of charged particles in an event. the particle pair with the lowest value of Y_{ij} is selected and replaced by a pseudo-particle with four momentum $(P_i + P_j)$. In successive steps the procedure is repeated until Y_{ij} are larger than a given jet cut resolution Y_{cut} . The resulting pseudo-particles are called jets. The choice of the lower limit for the scaled invariant mass has conventionally been set at $Y_{cut}=0.04$ for resolution of 4-jet.

With this jet definition, we get the case in window $|y| < 2.0$ as an example. See Fig.4, we can explain that the shoulder structure is formed by the superposition of 2-,3-,and 4-jet distribution. The shoulder is between $n=20$ and $n=25$ which is the overlap of the 3-jet peak and 4-jet peak. We can see in Fig.4, the peak of 2-jet distribution is at $n=8$, and for 3-jet distribution, it is at $n=13$, for 4-jet , it is at $n=20$.

4) Tab.4 lists the forward-backward multiplicity correlation strength b in different rapidity windows which has been given in our last note^[1]. We compare tab.2 with tab.4 carefully and found an interesting phenomenon. Seeing the fig.6 and fig.7, these two curves have the same turn-point at the $|y| < 0.5$. For strength b the turn point is the maximum point and for $\langle n \rangle / D$ it's a minimum point. This imply the relationship between the strength b and $\langle n \rangle / D$. The above results reveal the degree of the Poisson fit distribution, which shows the independence of emitted groups of particles, being narrower than real distribution. $\langle n \rangle / D$ value is a parameter which shows the narrow-wide property of multiplicity distribution. The distributions are narrower when the $\langle n \rangle / D$ value is bigger. The phenomenon shows that when strength is biggest the real multiplicity distribution is widest which means that the multiplicity distribution deviates more from Poisson-like. Thus, the more deviation from Poisson-like identifies the less independence of emitted particle and the more correlation. In this points, the strength b and $\langle n \rangle / D$ have the same inclusion and can be explained for each other.

4. Conclusions

© The multiplicity distribution has some characteristics of Poisson-like shape and is consistent with the corrected theoretical models, but is not good to fit to the data with standard Poisson shape, however, the fitting to 2-jet event multiplicity distribution is better than that of whole event.

⊙ The multiplicity distributions in intermediate rapidity windows (such as $|y| < 1.5$; $|y| < 2.0$) show a shoulder structure. This shoulder structure has been explained by mult-jet analysis.

⊙ Variation of $\langle n \rangle / D$ with rapidity intervals has opposite tendency with respect to the variation of multiplicity correlation strength b with rapidity intervals. This phenomenon implies that Poisson distribution shows the independence in particle emission, and the deviation from Poisson distribution consists with the F-B correlation strength b in different rapidity intervals.

References

- [1] Yi-Gang Xie, et al., ALEPH Collaboration, XXI International Conference on Multiparticle Dynamics(1991, Wuhan, China);
S. Huang et al., ALEPH Note 91-071, Physics 91-064,
Rapidity Dependence of Some Multihadronic Distributions and Parameters in e^+e^- Annihilation at LEP Energy
- [2] T. T. Chou and C. N. Yang, Proceeding of 25th International Conference on High Energy of Physics(Singapore), Vol II, P.1013,
Experimental Support for Geometrical Picture of Multiparticle Emission in e^+e^- Collision
- [3] P. Abreu et al., DELPHI Collaboration, Z. Physics C52(1991)271,
Charged Particle Multiplicity Distribution in Restricted Rapidity Intervals in Z^0 Hadronic Decays
- [4] D.Decamp, et al., ALEPH Collaboration, Phys. Lett. B234(1990)209,
Properties of Hadronic Events in e^+e^- Annihilation at $\sqrt{S}=91\text{Gev}$
- [5] D.Decamp et al., ALEPH Coll., Phys. Lett. B(273(1991)181,
Measurement of the Charged Particle Multiplicity Distribution in Hadronic Z^0 Decays.
- [6] A. Giovannini, S. Lupia, R. Ugoccioni, XXI International Conference on Multiparticle Dynamics(1991, Wuhan City, China),
Multiplicity Distributions in High Energy Collisions
- [7] S. Bashay(III. Physikalisches Institut Technische Hochschule Aachen, Aachen, Germany,
Possibility of Observable New Behavior for Multiparticle Production in e^+e^- Annihilation at LEP.
- [8] T. T. Chou and C. N. Yang Phys. Lett. B167(1986)453,
A Unified Physical Picture: Narrow Poisson-like Distribution for e^+e^- Two-jet Events and Wide Approximate KNO Distribution for Hadron-Hadron Collisions.
- [9] A. Capella, A. V. Ramallo, Phys. Rev. D37(1988)1763,
Are the e^+e^- and l-p Multiplicity Distributions Poissonian?

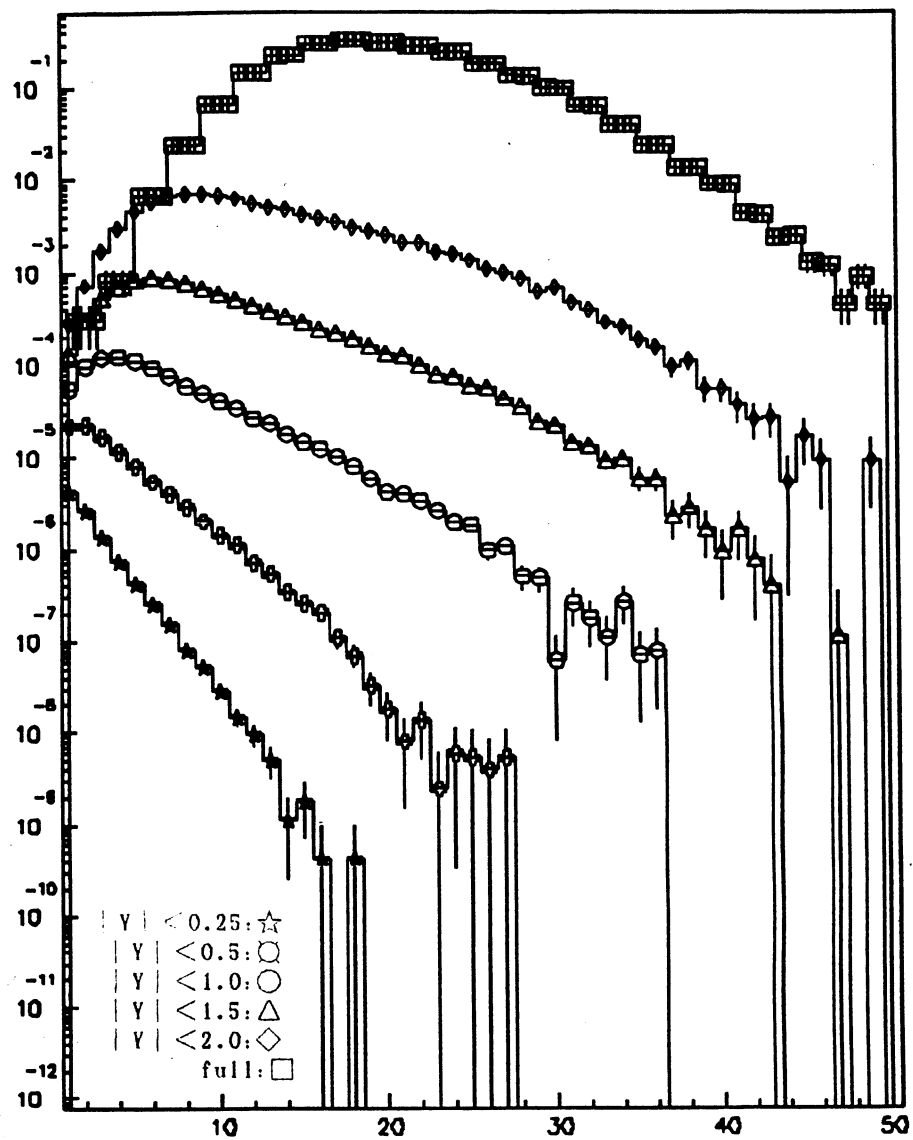


Fig.1 The charged particle multiplicity distributions of different rapidity window in full space.

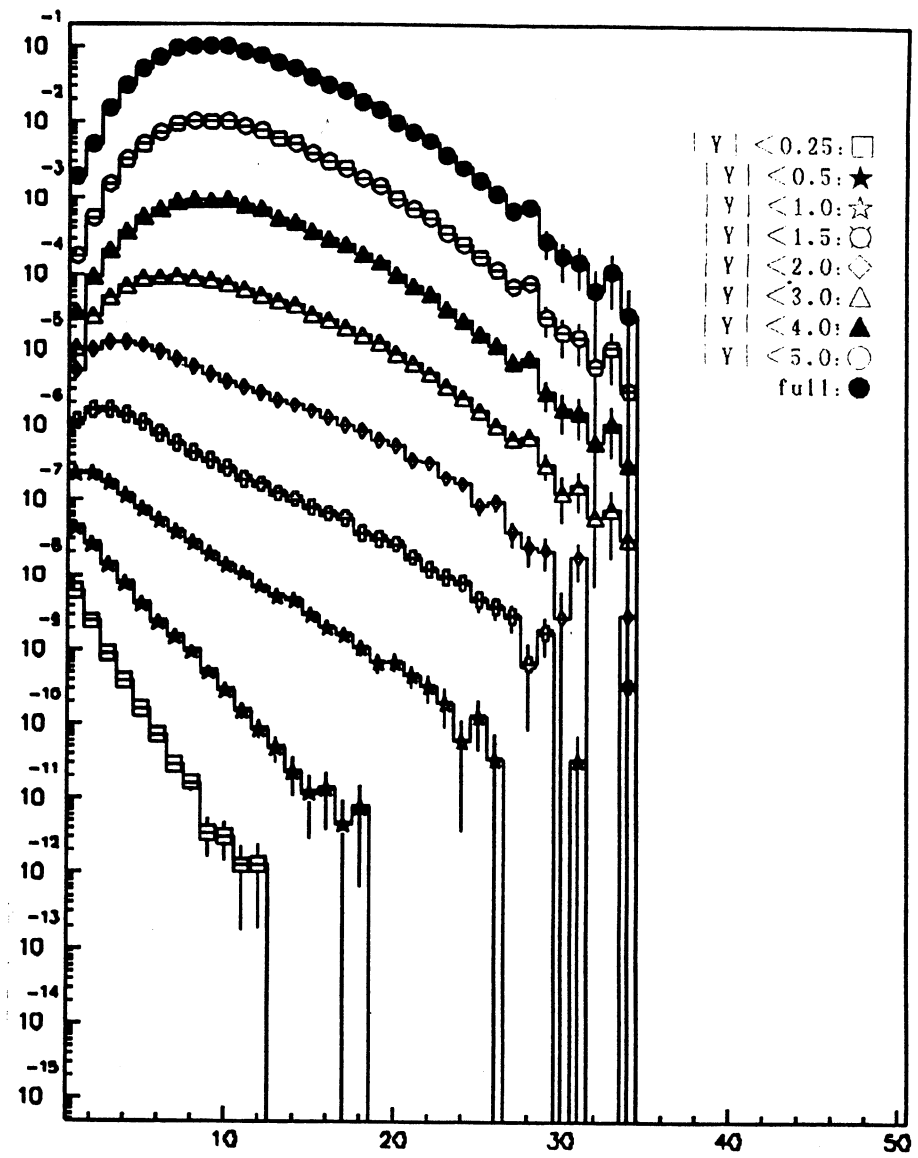


Fig.2 The charged particle multiplicity distributions of different rapidity window in single hemisphere.

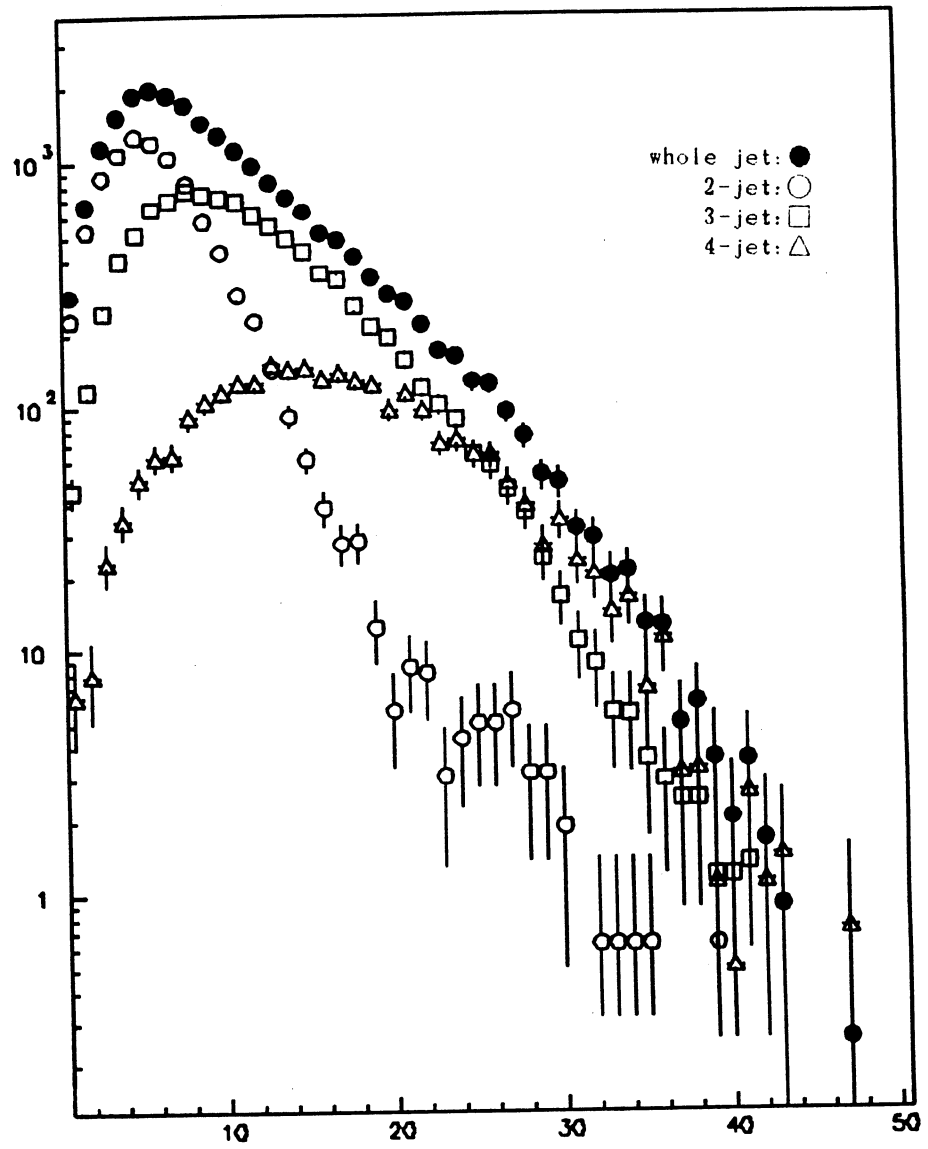


Fig.3 The charged particle multiplicity distribution of rapidity window $|Y| < 1.5$ in full space.

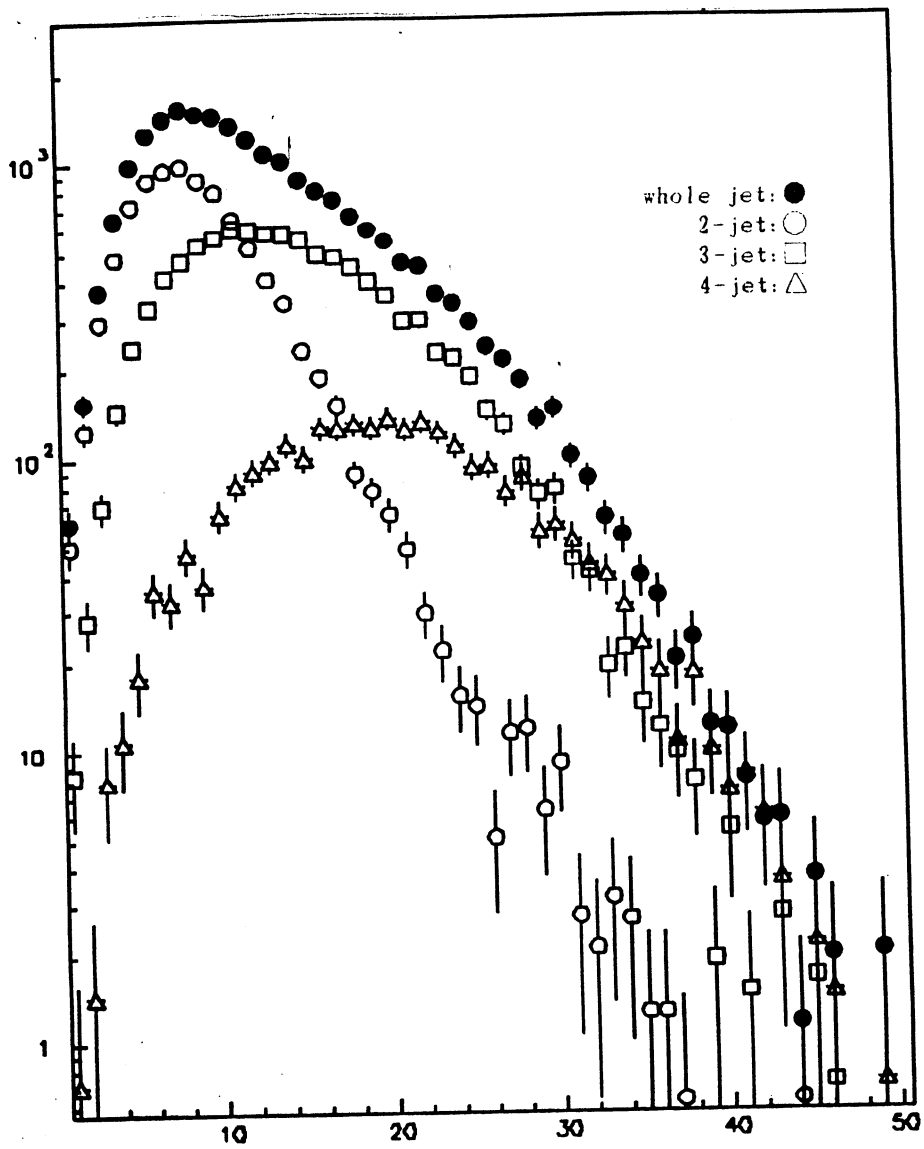


Fig.4 The charged particle multiplicity distribution of rapidity window $|Y| < 2.0$ in full space.

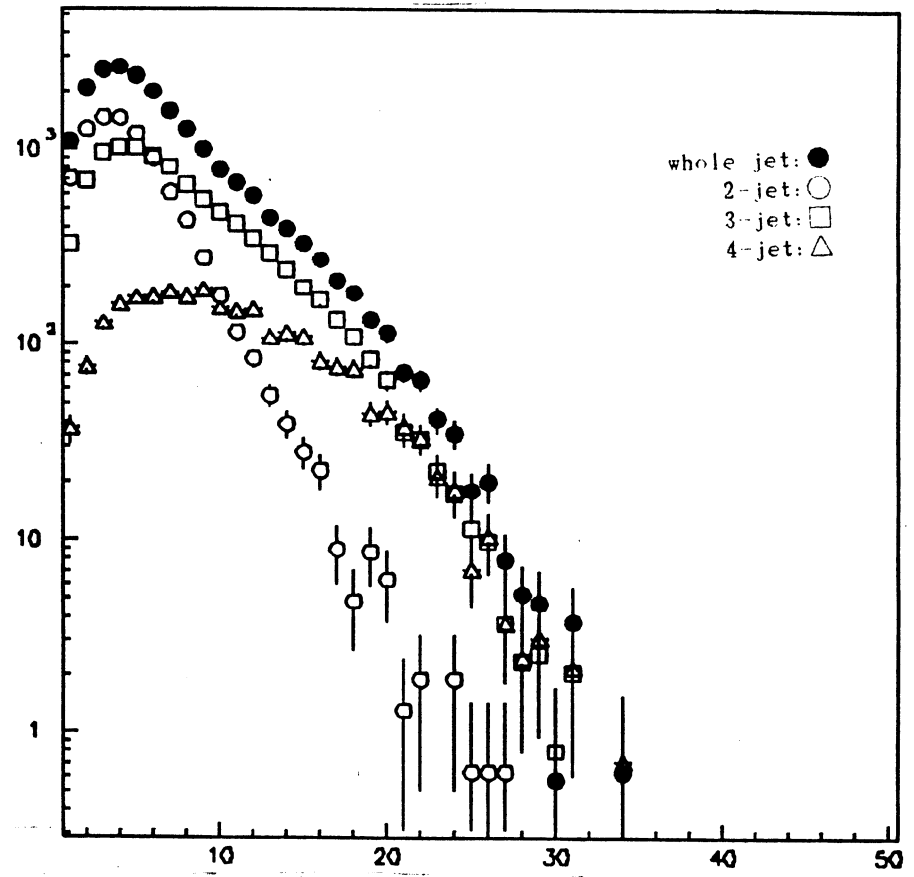
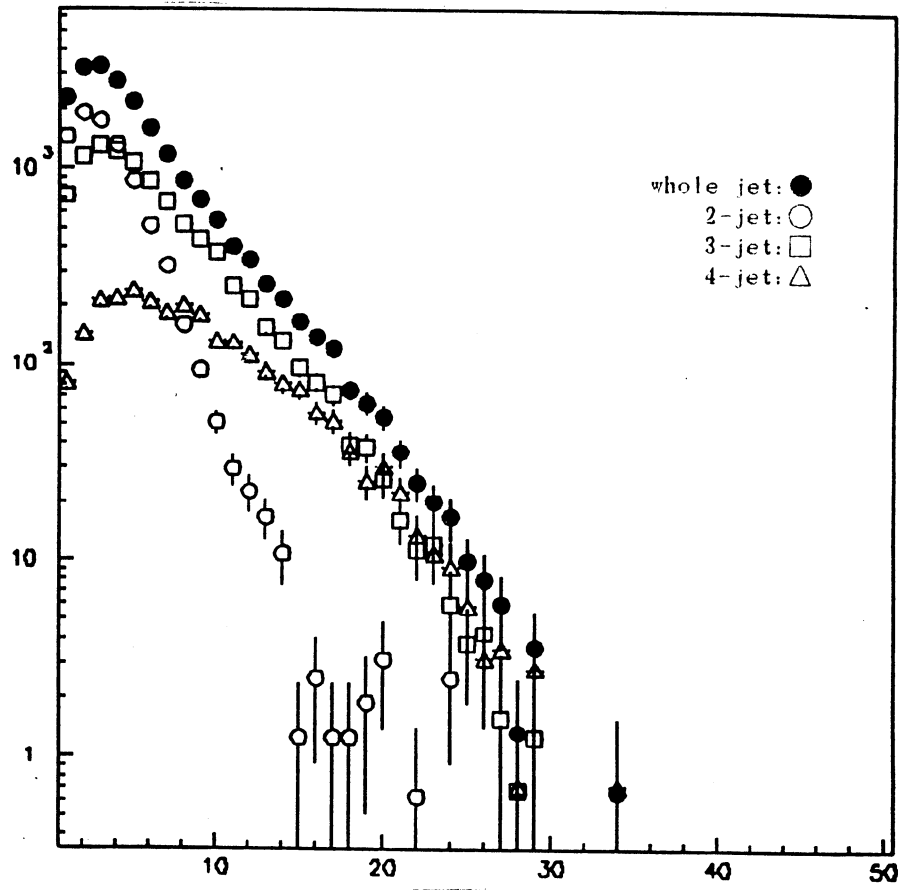


Fig.5 The charged particle multiplicity distribution of rapidity window $|Y| < 1.5$ (above) and $|Y| < 2.0$ (below) in single hemisphere.

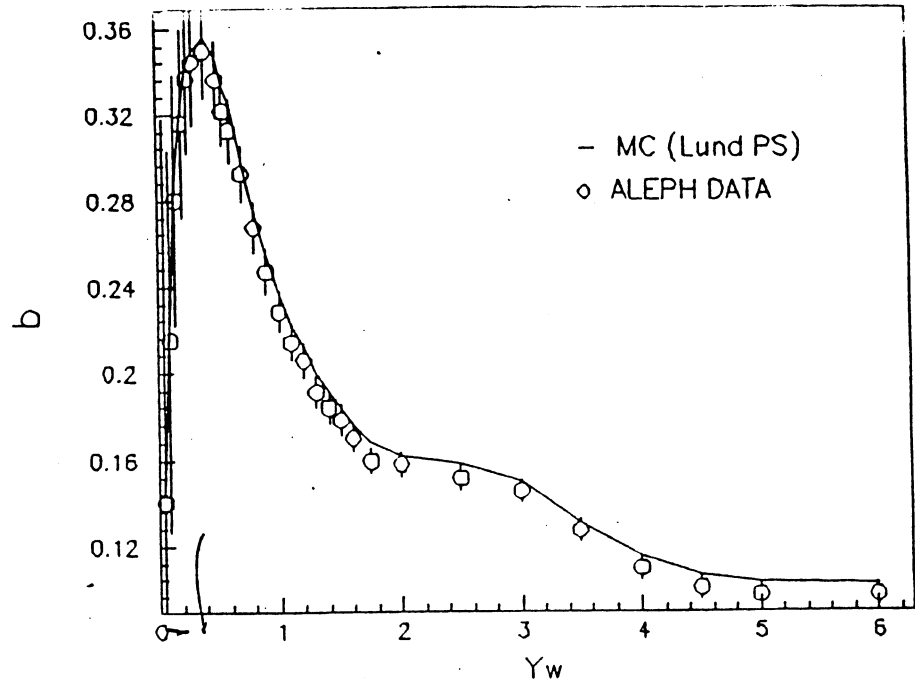


图5.8 前后向关联强度B随快度窗口的变化

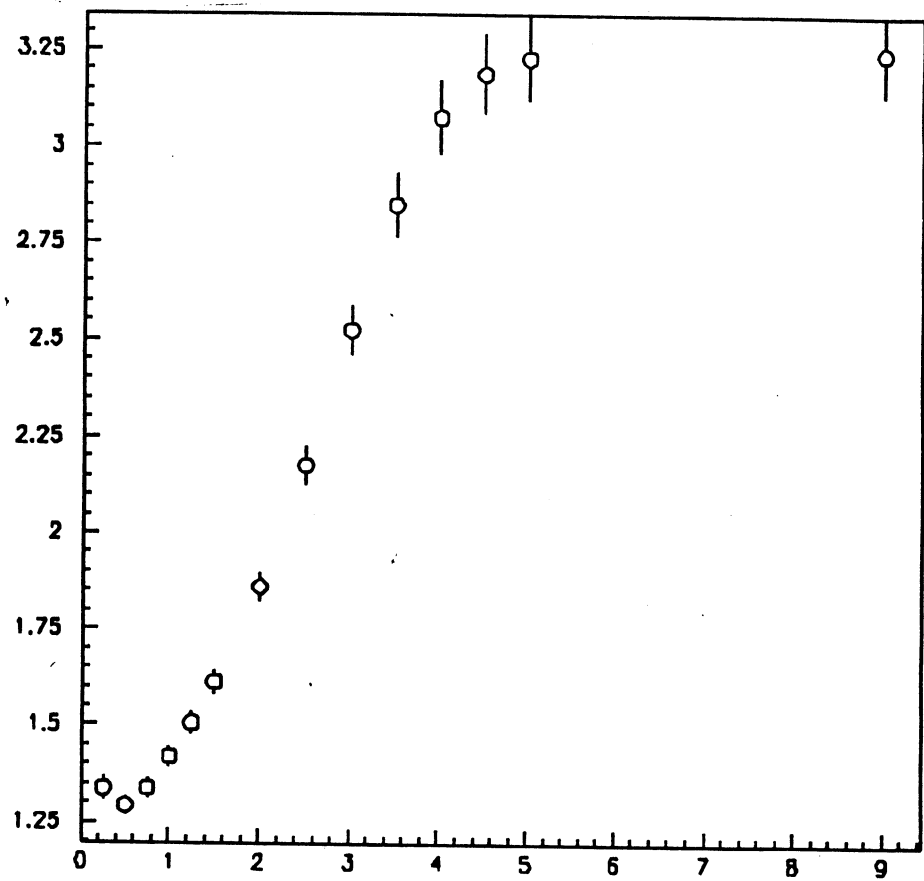


Fig.6(above) The multiplicity correlation strength(inclusive). Fig.7(below) The $\langle N \rangle / D$ of full space(inclusive).

Y	SINGLE HEMI.		BOTH HEMI.	
	<N>	ERROR	<N>	ERROR
0.25	1.669	0.011	2.307	0.014
0.50	2.311	0.014	3.655	0.020
0.75	2.972	0.018	5.109	0.027
1.00	3.654	0.021	6.668	0.032
1.25	4.368	0.025	8.248	0.037
1.50	5.109	0.027	9.857	0.042
2.00	6.589	0.031	13.060	0.048
2.50	8.000	0.033	15.965	0.050
3.00	9.121	0.032	18.264	0.049
3.50	9.823	0.031	19.693	0.047
4.00	10.189	0.030	20.431	0.045
4.50	10.332	0.030	20.717	0.044
5.00	10.376	0.029	20.805	0.044
9.00	10.390	0.029	20.835	0.044

Tab.1 The mean charged multiplicity of full space and single hemisphere.

Y	SING. HEM.	BOTH HEM.
	$\langle N \rangle / D$ ERR	$\langle N \rangle / D$ ERR
0.25	1.535 +-0.050	1.336 +-0.032
0.50	1.332 +-0.032	1.291 +-0.026
0.75	1.250 +-0.028	1.337 +-0.026
1.00	1.241 +-0.026	1.418 +-0.027
1.25	1.255 +-0.025	1.505 +-0.029
1.50	1.303 +-0.025	1.610 +-0.032
2.00	1.450 +-0.028	1.861 +-0.040
2.50	1.674 +-0.033	2.175 +-0.051
3.00	1.928 +-0.042	2.524 +-0.066
3.50	2.155 +-0.050	2.849 +-0.083
4.00	2.309 +-0.057	3.077 +-0.096
4.50	2.382 +-0.061	3.188 +-0.103
5.00	2.410 +-0.062	3.228 +-0.106
FULL	2.419 +-0.063	3.244 +-0.107

表5.3 $\langle N \rangle / D$ 的值

Y	$(\langle N \rangle / D)_f / (\langle N \rangle / D)_s$	ERROR
0.25	0.870	+ -0.047
0.50	0.969	+ -0.033
0.75	1.069	+ -0.027
1.00	1.142	+ -0.025
1.25	1.199	+ -0.023
1.50	1.236	+ -0.022
2.00	1.283	+ -0.022
2.50	1.299	+ -0.024
3.00	1.309	+ -0.026
3.50	1.322	+ -0.028
4.00	1.332	+ -0.030
4.50	1.338	+ -0.031
5.00	1.340	+ -0.031
full	1.341	+ -0.031

Tab.2 The $\langle N \rangle / D$ (above) and the ratio(below) of $\langle N \rangle / D$ in full space to $\langle N \rangle / D$ in single hemisphere.

SINGLE HEMI., WHOLE-JET EVENT			
Y	<N>	ERROR	χ^2/NDF
0.25	0.971	+0.015	40.4/11 = 3.67
0.50	1.631	+0.017	73.7/17 = 4.30
0.75	2.175	+0.019	99.6/21 = 4.74
1.00	2.710	+0.020	117.2/24 = 4.88
1.25	3.253	+0.022	122.7/27 = 4.54
1.50	3.834	+0.024	136.7/28 = 4.88
2.00	5.304	+0.030	157.9/30 = 5.26
2.50	6.594	+0.040	160.9/32 = 5.03
3.00	8.280	+0.044	142.1/32 = 4.44
3.50	9.265	+0.040	104.5/32 = 3.27
4.00	9.687	+0.036	79.03/32 = 2.47
4.50	9.835	+0.034	68.07/32 = 2.13
5.00	9.869	+0.033	64.29/32 = 2.01
FULL	9.879	+0.033	62.87/32 = 1.97

表 5. 5a 全喷注的单半球多重数泊松拟合

BOTH HEMI., WHOLE-JET EVENT			
Y	<N>	ERROR	χ^2/NDF
0.25	1.619	+0.017	86.4/15 = 5.76
0.50	2.762	+0.021	119.1/24 = 4.96
0.75	3.871	+0.025	145.2/28 = 5.19
1.00	5.063	+0.031	146.4/34 = 4.31
1.25	6.285	+0.038	148.2/38 = 3.90
1.50	7.598	+0.044	146.8/42 = 3.49
2.00	10.459	+0.055	150.8/46 = 3.28
2.50	14.105	+0.076	145.4/48 = 3.03
3.00	17.499	+0.037	233.3/99 = 2.36
3.50	19.252	+0.033	177.9/99 = 1.79
4.00	19.913	+0.030	142.9/99 = 1.44
4.50	20.155	+0.028	127.5/99 = 1.29
5.00	20.219	+0.027	124.7/97 = 1.22
FULL	20.244	+0.028	121.4/99 = 1.23

Tab.3a(above) The poisson fit of charged multiplicity distribution for whole jet event in single hemisphere. Tab.3b(below) The poisson fit of charged multiplicity distribution for whole jet event in full space.

SINGLE HEMI., 2-JET EVENT			
Y	<N>	ERROR	χ^2/NDF
0.25	0.498	+0.018	3.7/7 = 0.52
0.50	0.969	+0.018	4.9/11 = 0.45
0.75	1.454	+0.020	5.9/15 = 0.39
1.00	1.971	+0.021	9.5/16 = 0.59
1.25	2.525	+0.023	13.6/18 = 0.75
1.50	3.103	+0.026	19.6/19 = 1.03
2.00	4.287	+0.032	29.4/23 = 1.28
2.50	5.604	+0.039	36.5/26 = 1.40
3.00	6.965	+0.047	41.9/25 = 1.67
3.50	8.089	+0.046	28.4/27 = 1.05
4.00	8.689	+0.043	18.5/26 = 0.71
4.50	8.938	+0.040	11.9/27 = 0.44
5.00	9.013	+0.039	9.8/27 = 0.36
FULL	9.039	+0.039	9.1/27 = 0.34

表5.6b 2-喷注的单半球多重数泊松拟合

BOTH HEMI., 2-JET EVENT			
Y	<N>	ERROR	χ^2/NDF
0.25	0.921	+0.018	5.77/10 = 0.58
0.50	1.822	+0.020	7.01/17 = 0.41
0.75	2.761	+0.022	9.16/22 = 0.41
1.00	3.801	+0.027	13.02/25 = 0.52
1.25	4.891	+0.031	15.86/29 = 0.55
1.50	6.059	+0.036	20.55/31 = 0.66
2.00	8.592	+0.049	28.01/35 = 0.80
2.50	11.428	+0.06	34.78/38 = 0.92
3.00	14.354	+0.038	67.1/38 = 0.81
3.50	16.505	+0.037	52.42/85 = 0.62
4.00	17.559	+0.033	36.15/86 = 0.42
4.50	18.011	+0.031	28.81/86 = 0.34
5.00	18.166	+0.030	27.04/84 = 0.32
FULL	18.227	+0.029	26.15/85 = 0.31

Tab.3c(above) The poisson fit of charged multiplicity distribution for 2-jet event in single hemisphere. Tab.3d(below) The poisson fit of charged multiplicity distribution for 2-jet event in full space.

Y_w	MC		DATA	
$< Y_w$	b	CHI2/N _{df}	b	CHI2/N _{df}
0.05	0.1443±0.1746	0/ 2	0.1404±0.1773	0/ 2
0.10	0.2187±0.0875	0/ 4	0.2150±0.0888	0/ 4
0.15	0.2882±0.0578	1/ 5	0.2802±0.0589	1/ 5
0.20	0.3241±0.0433	1/ 7	0.3159±0.0439	2/ 7
0.25	0.3431±0.0347	2/ 9	0.3368±0.0354	2/ 8
0.30	0.3501±0.0289	4/10	0.3444±0.0296	3/10
0.40	0.3563±0.0219	10/13	0.3496±0.0223	10/12
0.50	0.3472±0.0176	19/15	0.3362±0.0180	20/15
0.55	0.3344±0.0160	27/16	0.3215±0.0164	24/15
0.60	0.3255±0.0148	33/18	0.3123±0.0151	27/17
0.70	0.2983±0.0128	43/20	0.2923±0.0131	32/20
0.80	0.2747±0.0113	66/22	0.2672±0.0115	54/22
0.90	0.2556±0.0102	89/24	0.2467±0.0104	70/23
1.00	0.2359±0.0092	100/24	0.2282±0.0095	79/24
1.10	0.2216±0.0086	121/26	0.2139±0.0088	102/26
1.20	0.2124±0.0080	140/25	0.2055±0.0082	116/25
1.30	0.2003±0.0075	162/26	0.1908±0.0077	128/26
1.40	0.1907±0.0071	179/26	0.1839±0.0073	139/26
1.50	0.1835±0.0067	173/26	0.1780±0.0069	118/26
1.60	0.1760±0.0065	186/26	0.1698±0.0066	137/26
1.75	0.1682±0.0061	190/26	0.1593±0.0062	139/26
2.00	0.1618±0.0057	182/26	0.1579±0.0058	145/26
2.50	0.1578±0.0055	167/26	0.1513±0.0055	143/26
3.00	0.1499±0.0055	124/26	0.1453±0.0055	106/26
3.50	0.1308±0.0057	71/26	0.1271±0.0057	68/26
4.00	0.1153±0.0059	40/26	0.1095±0.0059	42/26
4.50	0.1060±0.0060	29/26	0.1001±0.0060	31/26
5.00	0.1025±0.0061	27/26	0.0967±0.0061	24/26
6.00	0.1015±0.0061	26/26	0.0965±0.0061	25/26

Tab.4 Multiplicity correlation strength b ($|Y| < Y_w$, *inclusive*) w.r.t. sphericity axis).